In-situ Calibration Methods for Phased Array High Frequency Radars

Mael Flament (1) , Pierre J Flament (1) , Cedric Chavanne (1, 2) , Xavier Flores-Vidal (1, 3) , Isaac Rodriguez (3) , Louis Marié (4) and Tyson Hilmer (1, 5)

(1) University of Hawaii at Manoa, Honolulu, HI, United States (2) Institut des Sciences de la Mer de Rimouski, Oceanographie Physique, Rimouski, QC, Canada (3) Universidad Autonoma de Baja California, Instituto de Investigaciones Oceanológicas, Ensenada, Mexico (4) Ifremer, Laboratoire de Physique de l'Océan, Plouzané, France (5) OceanWaveS GmbH, Luneburg, Germany

Abstract. HF radars measure currents through the Doppler-shift of electromagnetic waves Bragg-scattered by surface gravity waves. While modern clocks and digital synthesizers yield range errors negligible compared to the bandwidth-limited range resolution, azimuth calibration issues arise for beam-forming phased arrays. Sources of errors in the phases of the received waves can be internal to the radar system (phase errors of filters, cable lengths, antenna tuning) and geophysical (standing waves, propagation and refraction anomalies). They result in azimuthal biases (which can be range-dependent) and beam-forming side-lobes (which induce Doppler ambiguities). We analyze the experimental calibrations of 17 deployments of WERA HF radars, performed between 2003 and 2012 in Hawaii, the Adriatic, France, Mexico and the Philippines. Several strategies were attempted: (i) passive reception of continuous multi-frequency transmitters on GPS-tracked boats, cars, and drones; (ii) bi-static calibrations of radars in mutual view; (iii) active echoes from vessels of opportunity of unknown positions or tracked through AIS; (iv) interference of unknown remote transmitters with the chirped local oscillator. We found that: (a) for antennas deployed on the sea shore, a single-azimuth calibration is sufficient to correct phases within a typical beam-forming azimuth range; (b) after applying this azimuth-independent correction, residual pointing errors are 1-2 deg. rms; (c) for antennas deployed on irregular cliffs or hills, back from shore, systematic biases appear for some azimuths at large incidence angles, suggesting that some of the ground-wave electromagnetic energy propagates in a terrain-following mode between the sea shore and the antennas; (d) for some sites, fluctuations of 10-25 deg. in radio phase at 20-40 deg. azimuthal period, not significantly correlated among antennas, are omnipresent in calibrations along a constant-range circle, suggesting standing waves or multiple paths in the presence of reflecting structures (buildings, fences), or possibly fractal nature of the wavefronts; (e) amplitudes lack stability in time and azimuth to be usable as a-priori calibrations, confirming the accepted method of re-normalizing amplitudes by the signal of nearby cells prior to beam-forming.

Acknowledgments: the HF radar processing software was provided by K-W. Gurgel, Universität Hamburg. Funding: DHS, ONR, NOAA, NSF, CoNaCyT.

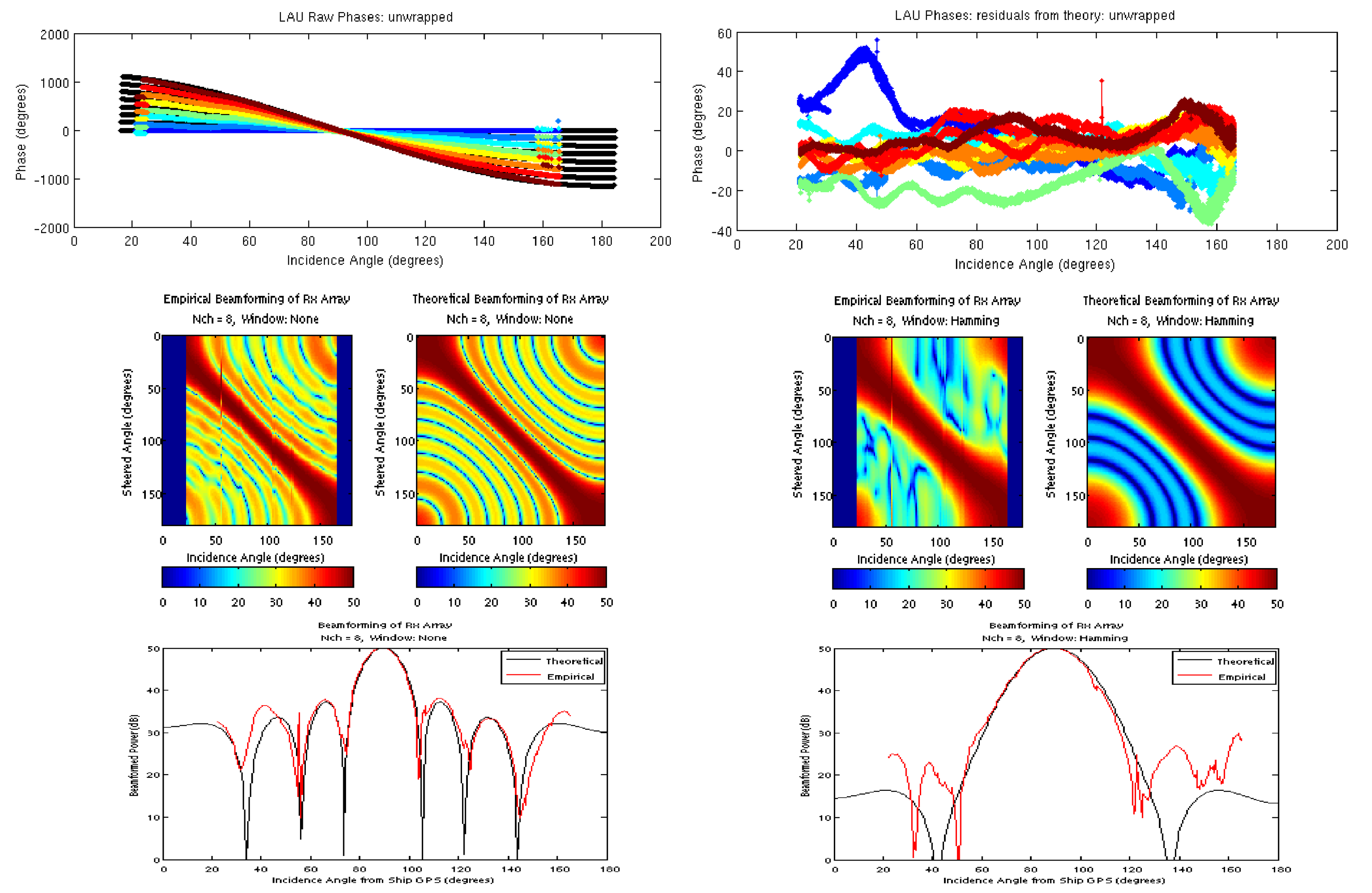

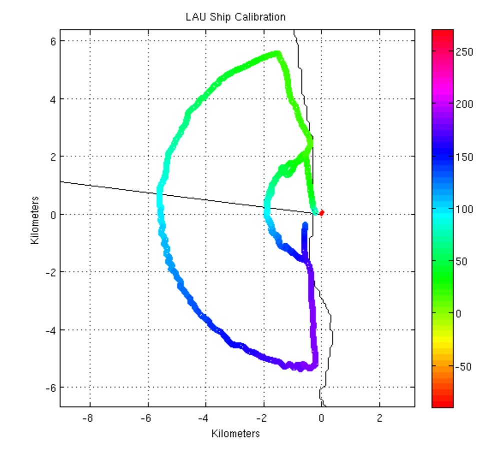

Calibration of phased array of 8 monopoles at 11.5 MHz in Lauan, Philippines. Bottom left: boat track. Top left: phases of antennas 2-8 referenced to antenna 1. Top right: residual phases with respect to the theoretical phase functions. Note the fluctuations of 10-25º in phase at 20-40º azimuthal period. Middle left: empirical and theoretical beamforming functions, using no azimuthal window. Middle right: same, using a Hamming window. Bottom right: GPS bearing of the boat vs. bearing inferred from beamforming. The internal calibrations of the input band-pass filters and receivers have been applied.

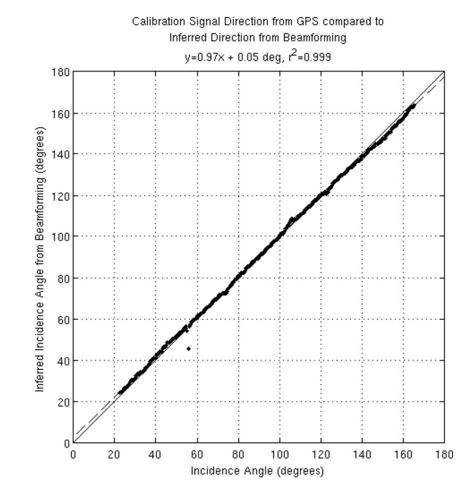

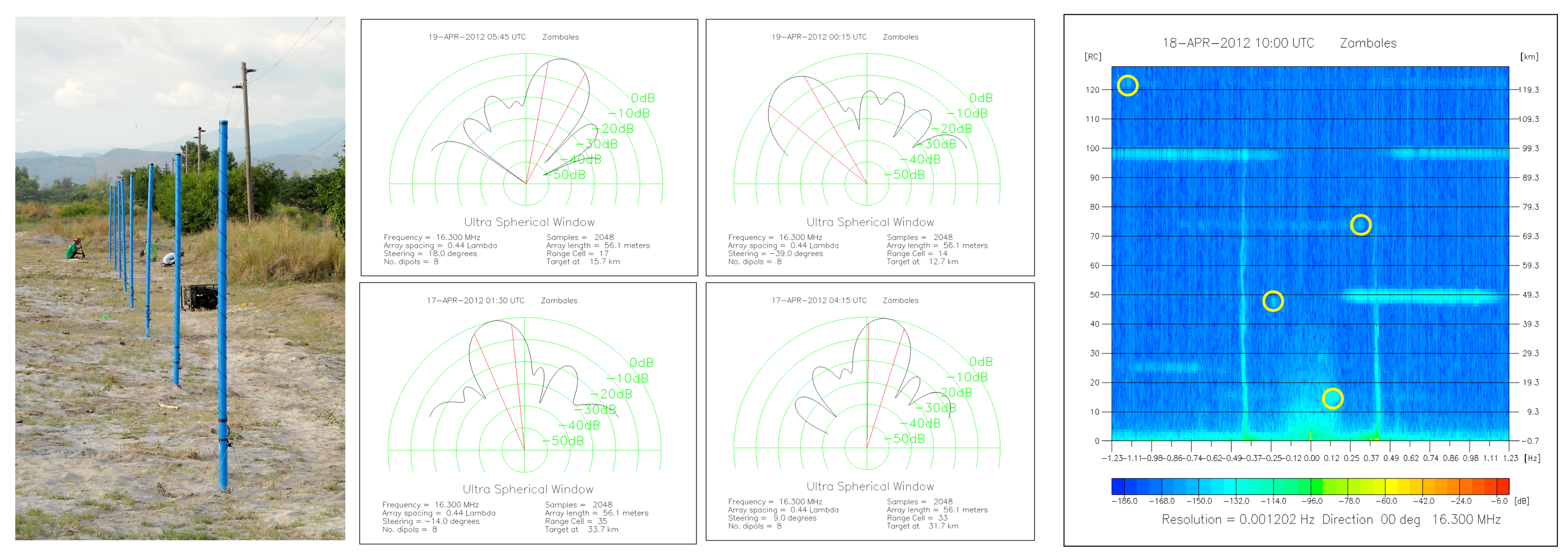

With well-tuned broadband monopoles antennas, and after applying phase corrections obtained from the internal calibrations of the input band-pass filters and receivers, the beam-forming array diagrams are generally very good, with side-lobes 15-20 dB below the main lobe up to 45º from the normal to the array, alleviating the need for further in-situ calibrations. Left: phased array of 8 monopoles at 16 MHz, Zambales, Philippines. Middle: examples of beam-forming array diagram for various targets of opportunity. Right: example of range-Doppler spectrum showing ship echoes.

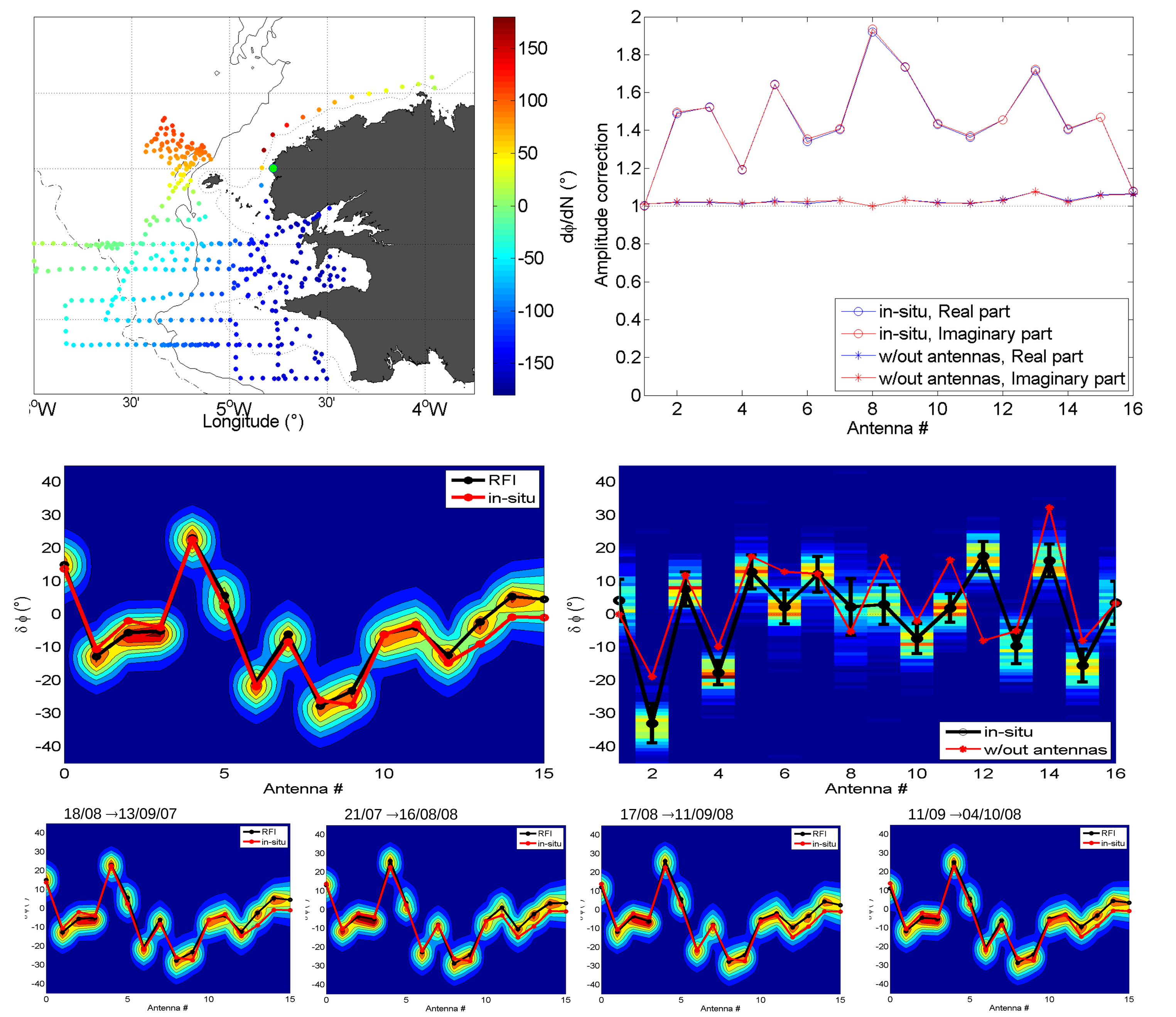

Top left: 1-min track of the R/V Côtes de la Manche, September 2008, carrying 12.5 MHz CW transmitter. Color is the mean phase difference between adjacent antennas in the north site Garchine. Top right: mean amplitude normalized by antenna 1, for ship transmission (0), and for internal receiver calibrations (*). Middle right: mean phases, for in-situ ship transmissions (black), and for internal receiver calibrations (red). Middle left: mean phases in south site Brézellec, for in-situ ship transmissions (red), and using opportunistic interference (RFI) transmissions (black). Bottom row: time series of mean phases using RFI (black) for different periods, showing the stability of the calibrations. The in-situ calibration during the cruise is shown for reference.
Adapted from Marié ,Thomas, Flament, Gurgel, Barbin, Arduhin, Gacg (2009).

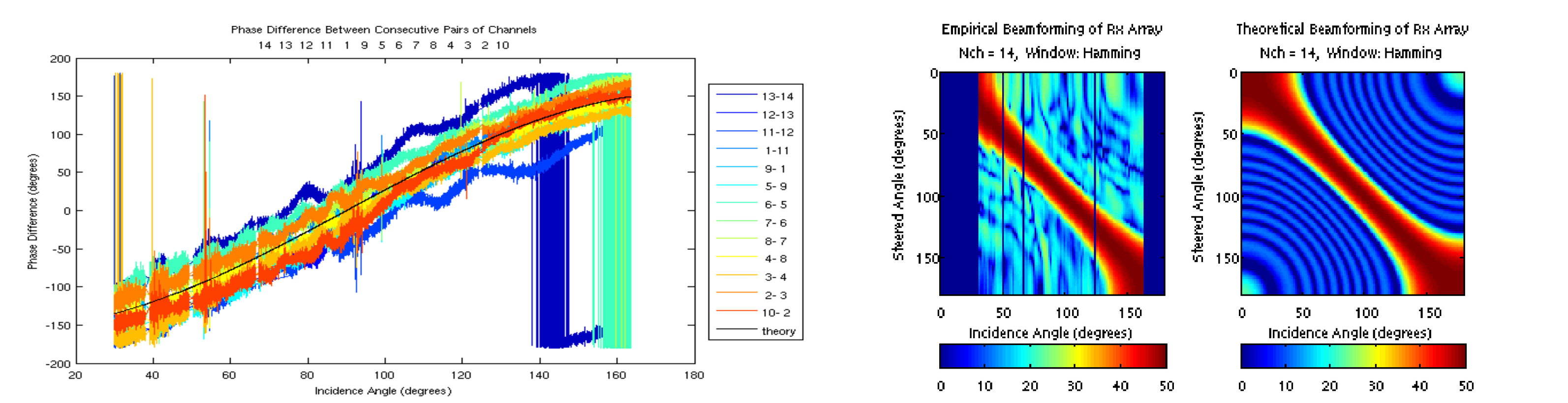

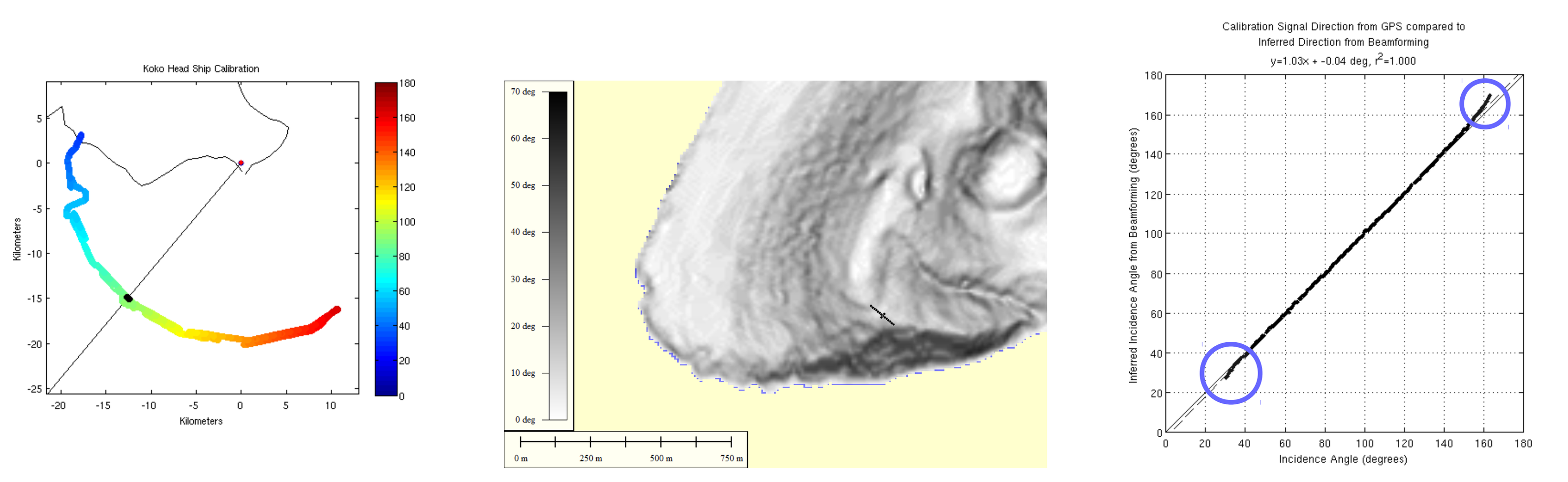

Calibration of phased array of 14 monopoles at 16.2 MHz in Koko head, Hawaii. Bottom left: boat track. Top left: relative phases of successive pairs of antennas. Note the fluctuations of 10-25º in phase at 20-40º azimuthal period. Top right: empirical and theoretical beamforming functions, using a Hamming window. Bottom right: GPS bearing of the boat vs. bearing inferred from beamforming. Note the increasing errors at large incidence angles (blue circles). Bottom middle: digital topography of the area; the receive antennas are deployed on a 200-m altitude crest. The internal calibrations of the input band-pass filters and receivers have been applied.

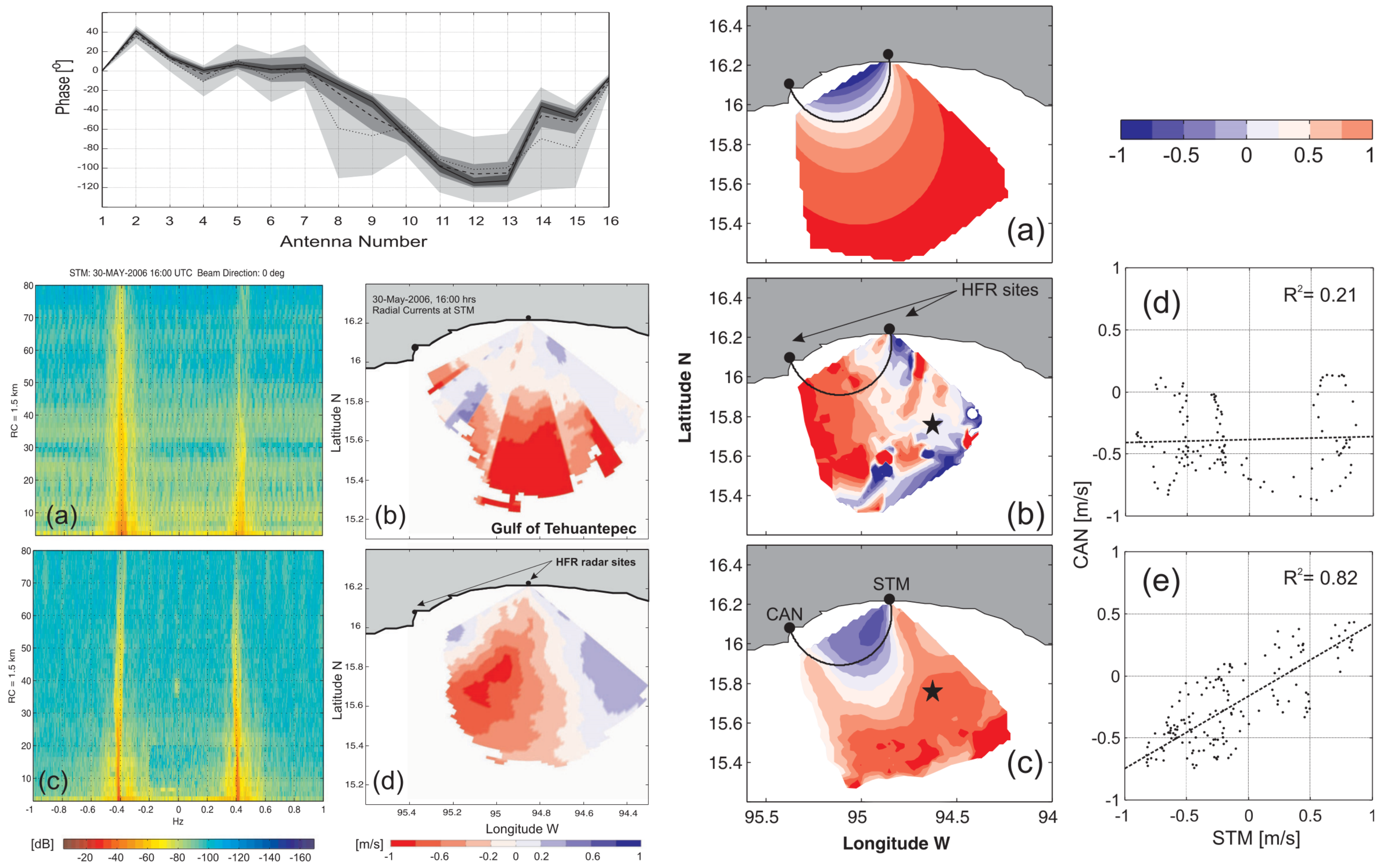

Damage to cables and undocumented repairs prevented beam-forming in Tehuantepec (16 MHz). Top left: 100 ship echoes spanning 3 years used to estimate channel phase corrections, including boot-strap errors based on 10, 50 and all echoes (shades). Middle left (a): spectrum beam-formed with no corrections have wide spread, due to side-lobe contaminations. Bottom left (c): applying corrections before beam-forming yield narrow-focused Bragg lines. Center (b): radial maps based on poorly beam-formed spectra respond erratically to side-lobes. Bottom center (d): applying corrections yield a well-defined radial field, typical of along-shore westward currents. Right: the normalized cross-correlation between sites is well-behaved only when corrections are applied (c) and mimics the cosine of the sites radials (a). With no corrections, the cross-correlation has no physical structure (b). The effect of calibration is shown by the scatter plot between radials, the correlation increasing from 0.21 to 0.82 when the corrections are applied.
Adapted from Flores-Vidal, Flament, Durazo, Chavanne and Gurgel (2013).

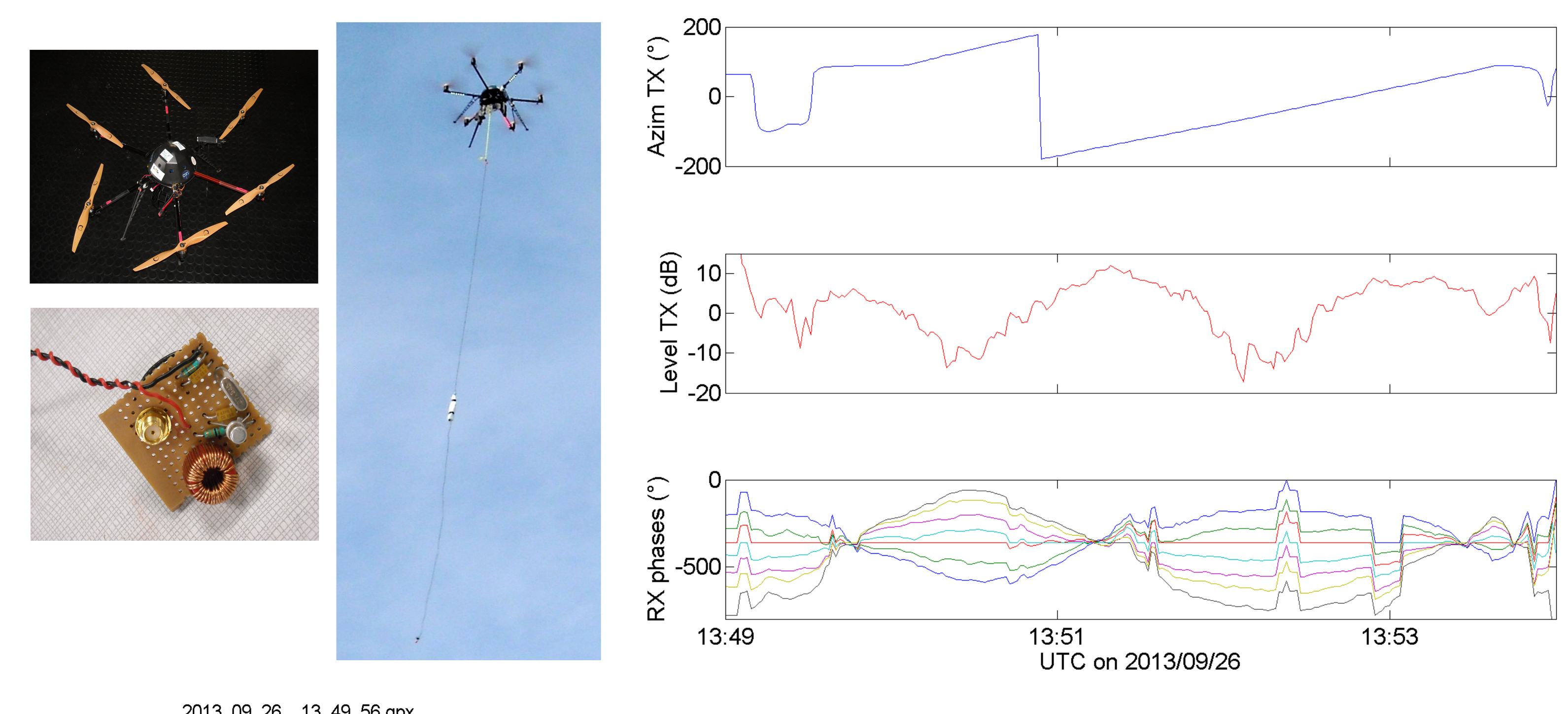

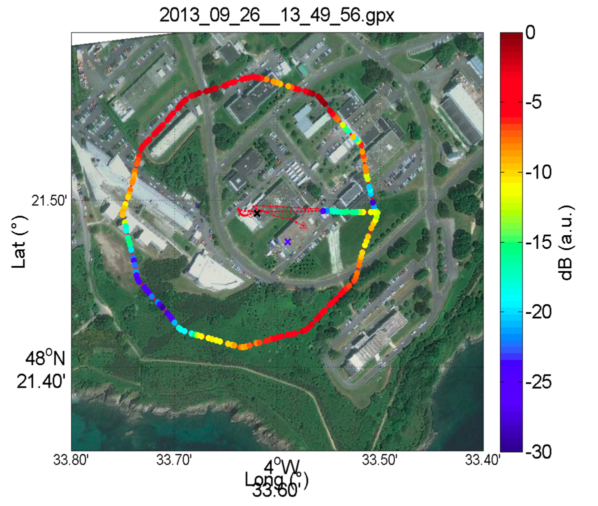

Top left: electrical hexacopter drone used for calibration of phased array of 8 monopoles at 27.5 MHz in Plouzane, France. Middle left: 27.5 MHz Crystal Oscillator. Top middle: drone in flight with λ/4 loaded dipole antenna (oscillator is at center of dipole). Bottom left: drone flight path, color-coded with amplitude of received signal; blue **X** shows the RX array oriented 135° and black **X** shows the TX array. Top right, time series of: (a) drone azimuth; (b) signal level using the 4-antenna beam-forming TX array as a receive array, to show the signal minima when the drone is aligned with the TX-RX direction; (c) phases of antennas 2-7 referenced to antenna 1, to show the convergence of phases when the drone is crossing the normal to the array, bearing 45° and 225°.